

CO₂ COMPRESSION AT WORLD'S LARGEST CARBON DIOXIDE INJECTION PROJECT

Antonio Musardo
Senior Project Engineer
GE Oil & Gas
Florence, Italy

Vinod Patel
Chief Technical Advisor
KBR
Houston, Texas

Gabriele Giovanni
Thermodynamic Senior Engineer
GE Oil & Gas
Florence, Italy

Marco Pelella
Centrifugal Compressor Engineering Manager
GE Oil & Gas
Florence, Italy

Mark Weatherwax
Senior Staff Machinery Engineer
Chevron ETC
Houston, Texas

Sergio Cipriani
Mechanical and System Engineer
GE Oil & Gas
Florence, Italy



Antonio Musardo is a Senior Project Engineer - Technologist for GE Oil & Gas Company, in Florence, Italy. His current responsibility is to assure the correct execution of large and complex LNG projects, coordinating engineering disciplines during design, manufacturing and final testing phase, supporting commissioning and start-up. Mr. Musardo joined GE Oil & Gas in 2001, in Testing Department following Field Test and String Testing activities, in 2005 he moved to the Project Engineering Area. Mr. Musardo graduated in Aeronautical Engineering at University of Pisa in 2000. He presently has one technical paper presented at Italian Aerospace Congress (AIDAA).



Vinod Patel is a Chief Technical Advisor, Machinery Technology, for KBR, in Houston Texas. In his assignment, he is responsible in preparation and auditing of specifications, equipment evaluation, engineering coordination, and testing and installation start-up of rotating and special equipment. He has worked in various applications of rotating machinery in the petrochemical and refinery processes including ammonia, LNG, olefins, cat-cracking, and hydrotreating for domestic and international projects. Mr. Patel has B.S. and M.S. degrees in Mechanical Engineering from Maharaja Sarajirao University and Youngstown University, respectively. He is a Professional Engineer in the State of Texas



Mark Weatherwax is a Staff Machinery Engineer for Chevron Energy Technology Company, in Houston, Texas. His current responsibilities include providing technical assistance with the selection, design, specification and testing of new equipment along with start-up, commissioning and troubleshooting support for existing equipment. Mr. Weatherwax has more than 20 years of experience with rotating equipment. Prior to joining Chevron in 2006, he was employed by M.W. Kellogg and Ingersoll-Rand. Mr. Weatherwax has B.S. and M.S. degrees in Mechanical Engineering from Texas A&M University and is a Professional Engineer in the State of Texas.



Marco Pelella is Engineering Manager for Centrifugal Compressor LNG and Downstream Applications with GE Oil & Gas in Florence, Italy. He also holds the title of Senior Engineer. His responsibilities include the thermodynamic and rotordynamic study of centrifugal compressors as well as their stress verification and material selection. Mr. Pelella graduated in Mechanical Engineering at University of Naples in 1997. He joined GE in 1999 as Design Engineer in Centrifugal Compressor Requisition team, then he has worked as Requisition Team Leader of integrally geared and pipeline compressors, Requisition Manager in Le Creusot (France) for centrifugal compressors of low and medium pressure in normal and sour services. He presently holds 3 patents.



Giovani is Engineering Manager for Engineering Process and Tools organization. He also holds the title of Senior Engineer for thermodynamic. His responsibility covers the development and maintenance of Technical Tools for the selection, performance computation and mechanical analysis of centrifugal and reciprocating compressor, steam turbine and turbo-expander leveraging the fundamental disciplines like thermo-aerodynamic, mechanic, software and analytic. Mr. Giovani graduated in Mechanical Engineering at University of Bologna in 1996. He joined GE in 1998 mainly focused on engineering tools development and thermodynamic process applied to turbo-machine. He has developed a thermodynamic model for geothermal steam and performed several experimental researches on sour gas. He moved in 2008 in centrifugal compressor tools team as project leader for the new stage introduction and later for the automation and selection of centrifugal compressor train. He was appointed Technical Tool manager in 2011.



Sergio Cipriani is a Lead System for GE Oil & Gas Integrator Engineering for Gas Turbine and Centrifugal Compressor auxiliary systems with GE Oil & Gas in Florence, Italy. He is responsible for the design and integration of gas turbine and moto-compressor critical equipment and systems, through P&ID design and management of project specifications and design of all critical auxiliaries. Mr. Cipriani graduated in Mechanical Engineering at University of Florence in 2006. He joined GE in 2006 as Mechanical Engineer in Gas Turbine and Centrifugal Compressor auxiliary requisition team, and he has changed as System Integrator on 2009.

ABSTRACT

Compressors for carbon dioxide (CO₂) applications have been widely used in the O&G industry for urea production, enhanced oil recovery (EOR) and CO₂ pipeline services for many years.

New environmental challenges have re-focused the attention on increasing the efficiency of rotating equipment including optimization of the equipment configuration.

To address these challenges, an electric motor driven CO₂ compressor train has been designed for a large CO₂ injection project in Western Australia. This compressor train was equipped with two compressor casings coupled through two gearboxes on either side of a double-ended variable frequency drive (VFD) motor.

For the CO₂ injection project, the risk of condensation inside the carbon steel pipeline between compressor discharge and the injection wells was identified as a concern. The mixture of liquid water and CO₂ results in carbonic acid that may result in corrosion of the carbon steel pipeline. To mitigate this risk

the water needs to be removed from the CO₂ stream prior to entering the pipeline. To maximize the removal of water, the CO₂ compressor intermediate stage (3rd stage) pressure is required to operate within a fixed pressure range.

The compressor string with two gearboxes, two compressor casings and a VFD results in a complicated torsional system. In cases where torsional vibration frequencies coincide with resonance frequencies, large torsional deflections and internal stresses could be generated.

Continuous operation under these conditions could result in fatigue failure. Free-vibration analysis and a forced-response analysis were conducted for an analytical review of rotor response to static and harmonic torsional loads.

VFD motors generate pulsating torques; even if the pulsating torques are very small with respect to the main torque, they can excite compressor train resonances with potential shaft and/or couplings damages.

Final validation of the compressor trains has been the Full Speed, Full Load test and ASME PTC10 Type 1 performance test campaign conducted in June 2011. During this testing, torque pulsation measurements has been conducted for validation of torsional analytical results and pulsation amplitudes under steady state and start-up conditions.

The compressor train was designed to be modularized. This required the package's overall dimensions to meet very stringent space constraints.

The project engineering challenges include: ergonomic design focusing on improving maintenance and operations access, compressor supports stiffness analysis for installation on module steel work and compressor train operability assessment.

High CO₂ discharge pressures, high operating temperatures and the need to minimize fugitive emissions result in challenges for the dry gas seals system (DGS) and lead to the design of a highly customized DGS configuration.

INTRODUCTION

CO₂ process compressors are mostly used in applications such as fertilizer plants, CO₂ pipelines, carbon capture and storage, and EOR.

The first two are well established applications, while the latter two are more recent. In any case, there are commonalities among all four. Understanding CO₂ gas properties, interaction with the compression process and OEM experience can bring an added value to the development of these new frontiers.

The OEM has supplied more than 200 compressors for CO₂ applications since 1971. Most of the applications have been for fertilizer and urea process plants where carbon dioxide is combined with ammonia to form urea, which is used as an agricultural fertilizer. The typical pressure required by the process is close to 2900 psi (200 bar). A similar pressure is also typical of carbon capture and storage (CCS) and EOR. For CCS, the CO₂ is injected and stored in subsurface geological formations. Unlike the fertilizer and urea process plants, CCS and EOR applications may have incidental associated substances such as hydrogen sulfide (H₂S) in the CO₂. The presence of H₂S increases the complexity of the compressor material and seal selections. The material selection is critical

due to two factors:

- Presence of H₂S leads to Stress Corrosion Cracking;
- Risk of rapid depressurization resulting in low temperatures, -130°F (-90°C).

The material selection aspects are addressed later in this paper. In general, CO₂ compressor typologies can be barrel or integrally geared type compressors. The authors are currently designing and manufacturing the compressors for the world's largest CO₂ injection project to be installed in the Chevron operated Gorgon Project – a LNG and domestic gas facility being constructed on Barrow Island off the north-west coast of Australia.

The Gorgon Project is a joint venture of the Australian subsidiaries of Chevron (approximately 47 percent), ExxonMobil (25 percent), Shell (25 percent), Osaka Gas (1.25 percent), Tokyo Gas (one percent) and Chubu Electric Power (0.417 percent).

The Australian Government has committed \$60 million to the Gorgon Project as part of the Low Emissions Technology Demonstration Fund (LETDF).

CO₂ injection is being incorporated into the Gorgon Project to reduce overall greenhouse gas emissions. CO₂ will be injected into an underground reservoir at a depth of approximately 8202 feet (2500 m) and a pressure close to 2900 psi (200 bar).

Barrel compressors are used for both LP and HP sections, with the driver between the two to facilitate bundle removal. Each compressor body includes two compression stages to result in four stages of compression. The compressor skids are being installed in compression modules prior to shipment to site.

OVERVIEW OF THE PROCESS

LNG facilities are supplied with natural gas from offshore wells. The raw natural gas comprises predominantly methane but includes minor amounts of water, condensate, CO₂ and H₂S that are removed prior to liquefaction. The first step in the gas processing operations is the removal of any liquid water and condensate in a slug catcher.

The gas stream leaves the slug catcher and enters an acid gas removal unit (AGRU). The AGRU utilizes an activated methyl diethanolamine (amDEA) solvent to remove the CO₂ and H₂S from the gas stream prior to the gas proceeding into the LNG liquefaction process.

The CO₂ and H₂S gas mixture leaves the AGRU at approximately atmospheric pressure and contains traces of hydrocarbons and is water saturated.

To allow the use of a carbon steel high pressure pipeline, the Gorgon CO₂ injection facility has been designed to control the 3rd stage discharge pressure to within the range of 725-943 psi (50-65 bar) to allow the maximum dropout of liquid water.

During a shutdown, the pipeline will remain liquid water free even if the pipeline pressure is blown down to atmospheric pressure and the site is at minimum ambient temperature.

The compressor, however, will have saturated gas mixing from the first 3 stages (prior to the water removal) and therefore the entire compressor has been designed with corrosion resistant materials suitable for free water and CO₂ during a

shutdown event.

COMPARISON WITH INTEGRALLY GEARED COMPRESSORS

During the early phases of the project, a review was made to determine the appropriate compressor design for the Gorgon CO₂ compressors (Figure 1). The two types of compressors found to be applicable for this service were conventional beam type compressors and integrally geared compressors.

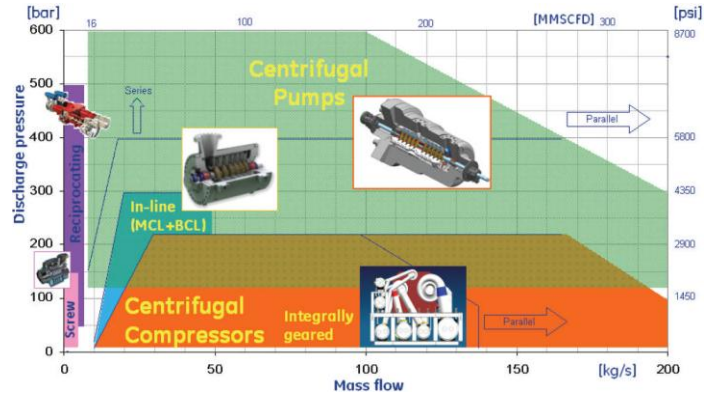


Figure 1. Technology Map

The following considerations were made in determining the final selection.

- Safety aspects with CO₂ and H₂S, specifically with regard to the available sealing technologies.
- Maintainability and maintenance access (ergonomics).
- Machine complexity.
- Intercoolers using air coolers instead of water coolers.
- Nozzle loads with cyclonic wind conditions.
- Overall power consumption for CO₂ injection.

At the time of the compressor technology reviews, the integrally geared compressors used in comparable high pressure services utilized carbon ring seals. The carbon rings seals are referenced back to lower pressure stages to prevent leakage. During a shutdown, the casings will reach the same settle-out pressure, and the seals will leak to the atmosphere unless the unit is depressurized. Fast depressurization is a concern for CO₂ because of the formation of solid CO₂ (dry ice). Considering the compressors were being located in modules and the process gas contains minor amounts of H₂S, it was determined that DGS were required for the application for safety considerations. The conventional beam type compressor arrangement consists of two compressor bodies and therefore 4 DGS. The integrally geared option requires a minimum of 8 compressor stages and therefore 8 DGS.

Ergonomic design is an important Gorgon Project goal for the plant operators and maintenance personnel. This will improve the safety aspects for maintenance/operation and enhance the overall plant operability and reliability. The conventional beam type compressor can be designed to improve access to bearings, seals and rotating assemblies.

The barrel type compressor arrangement selected does not require the process piping to be removed for normal

maintenance activities.

Integrally geared compressors require removal of suction piping, head covers and impellers to access DGS, and removal of discharge piping, stage casing and upper half of the gear box casing to access journal bearings.

From a safety standpoint, the HP barrel compressor has been designed with only one head-cover (3rd suction side) while the 4th stage head-cover is integral with casing and avoids the risk of high pressure leakage. The integrally geared option needs head-covers with relevant sealing gaskets on all 8 stages.

The class of CO₂ compressors used for this application are complex regardless of the type of compressor chosen. The barrel compressors are each located on opposite ends of a double ended VFD (Figure 2).

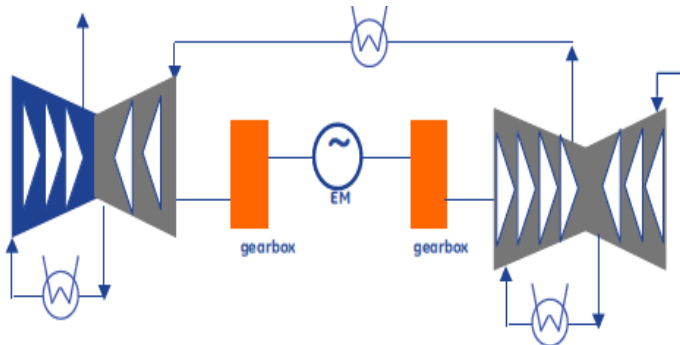


Figure 2. CO₂ string configuration

Both compressors utilize a speed increasing gear between the compressor body and the motor. This arrangement, utilizing a VFD, results in complex torsional and lateral interactions that will be discussed further in this paper. Similarly, 8 stage integrally geared compressors are complex mechanical assemblies with 4 pinion gears and variable inlet guide vanes on multiple compressor stages.

For the Gorgon facility, the stage inter-cooling is performed with air coolers. With the conventional (barrel) machine design there are 4 compression stages utilizing 3 inter-coolers and one after-cooler. These coolers are located on the top level of the modules. When integrally geared compressors are considered, more inter-coolers are utilized to fully achieve the increased efficiency and reduced compression power. Integrally geared compressors lend themselves to water cooled facilities so the inter-stage piping and associated pressure drops can be minimized by locating the inter-coolers very close to the compressor. For the Gorgon Project, the use of water cooling was not an option, and therefore, the increased pressure drop between stages for air coolers and piping diminishes the overall efficiency gains from the integrally geared option.

The Gorgon Project facility on Barrow Island is located off the coast of Northwest Australia in an area prone to tropical cyclones. As such, the facility is designed to withstand cyclonic wind loads and operate through major storm events. The barrel types compressor casings are more suitable to withstand the large nozzle loads that result. The design basis for the compressors is to handle up to 20 times the NEMA flange loads.

Integrally geared compressors with the scroll connected to the gear casing do not lend themselves to the same levels of

flange loading.

The overall efficiency is higher for the integrally geared options resulting in lower compression power. This improved efficiency results from the ability to optimize each pinion speed for maximum stage efficiency and utilize more stages of inter-cooling. The requirement for air cooling and the location of the inter-coolers increased the inter-stage pressure losses. The increased inter-stage pressure loss minimizes the overall efficiency improvements between the two options. In addition, at the time the compressor type selections were made, integrally geared compressors were not referenced for a combination of the flows and discharge pressures required for the Gorgon CO₂ injection application.

The final result of the review was to select the barrel type compressor primarily due to the ability to minimize the number of seals, improve the maintenance access and to accommodate the cyclonic wind conditions that would be experienced at site.

THERMODYNAMICS

Although CO₂ has been used for urea synthesis plants since 1922¹, and centrifugal compressors have been successfully applied for this application for over 30 years, experimental data for the CO₂ gas mixture (including other components like H₂S, hydrogen, oxygen, methane and especially water) is not available.

The OEM decided to invest in a comprehensive test campaign covering CO₂ gas mixtures in order to identify the best Equation of state (EOS) to be applied for each application.

Experimental measurements for Density, Speed of Sound and Specific Heat at constant volume

The most important thermodynamic properties for the prediction of centrifugal compressor performance are density, SoS and specific heat (Cp and Cv). Density and Speed Of Sound (SoS) impact both the selection of impellers (flow coefficient and peripheral Mach number), while specific heat impacts all energetic quantities (enthalpy, internal energy). Specific heat at constant pressure (Cp) is directly linked to enthalpy and therefore directly impacts the performance of centrifugal compressors. Specific heat at constant volume (Cv) is linked only to internal energy. Due to the technical difficulties in measuring specific heat at constant pressure (it requires an open thermodynamic system) it was decided to measure specific heat at constant volume.

Test Results

A test campaign was defined using a typical CO₂ gas mixture applied in the urea synthesis plant and EOR. It also included a particular composition in order to expand the measurement on a very wide region of the thermodynamic plane. Overall, the test campaign covers a pressure range from 16.2 psi (1.12 Bar) to 9065 psi (625 bar) and a temperature range from 95°F (35°C) to 464°F (240°C). Particular focus has been put on the supercritical region at very high temperatures as well as around the critical isotherm.

The choice of the EOS has been selected according to the

OEM experience in this type of application. A conservative approach was taken in deciding to use the BWRS Equation of state.

The BWRS Equation of state is one of the most recommended¹

for CO₂ even if new and very promising Equations of state, like GERG 2008 or MBWR, are now available.

This is due to the successful use of the BWRS over the past 30 years in similar applications and limitations of other EOS (e.g. MBWR can be applied only for pure CO₂).

¹ R. Span, W. Wagner. "A new Equation of State for Carbon Dioxide Covering the Fluid region from Triple point temperature to 1100k at pressures up to 800 Mpa"; Journal of Phys. Chem. Ref. Data, Vol. 25, No. 6, 1996

The OEM started its massive test campaign in 2009 in order to validate and select the best thermodynamic models. Figure 3 shows the plot of the differences between experimental data and computed values as functions of the pressure, density, speed of sound and specific heat at constant volume. Differences are contained mainly in the range ± 1% except few isolated cases due mainly to uncertainty in the measure (relatively big variation during repetition of the tests).

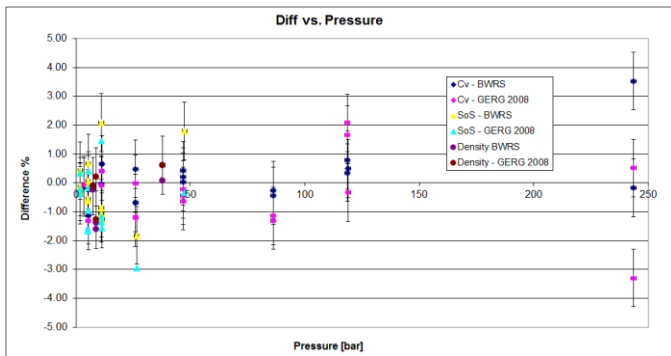


Figure 3. Comparison of Differences between experimental vs. computed value of Density, Speed of Sound and Specific Heat constant volume

CO₂ ANALYSIS RESULTS

CO₂ has a critical pressure and temperature of approximately 1073 psi (74 Bar) and 88°F (31 °C) respectively. For comparison purposes, methane (CH₄) has a critical pressure and temperature of approximately 667 psi (46 bar) and -117°F (-83 °C) respectively. In this application, it is likely to operate the 3rd stage discharge of the compressor at conditions close to 1073 psi (74 bar) and the ambient temperatures can potentially be in the range of 88°F (31°C). Operating in close proximity to the critical point for CO₂ results in very large changes in density of the gas as it enters the 4th stage compressor. Small changes in temperature result in significant changes in the density at constant pressure (Figure 4). Similar changes occur for the compressibility factor Z with changes in temperature.

For this reason the Gorgon Project has incorporated temperature control on the 3rd stage inter-cooler.

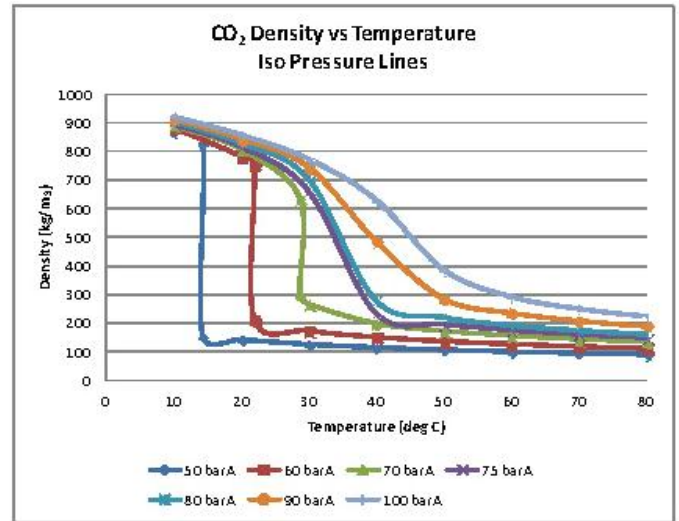


Figure 4. CO₂ Density Variation vs Temperature

AERODYNAMICS

The Gorgon CO₂ compressor operating parameters for the design case are in the Table 1 below shown:

Table 1. CO₂ Compressor operating parameters (Note: an operating case can deliver up to 3147 psi (217 bar)).

	LP Casing		HP Casing	
	1	2	3	4
VOLUME FLOW (m ³ /h) (10 ³ BAR-A & 0°C DRY)	5407	5407	5407	5407
WEIGHT FLOW, (kg/h) (WET)	103397	105829	101116	104396
INLET CONDITIONS				
PRESSURE (BarA)	178	5,80	23,42	57,33
TEMPERATURE (°C)	45,7	44,0	44,0	44,0
RELATIVE HUMIDITY %	100,0	100,0	100,0	100,0
MOLECULAR WEIGHT	42,56	43,61	43,91	43,97
C _p /C _v (K ₁) OR (K _{AVG})	1289	1308	1423	1955
COMPRESSIBILITY (Z ₁) OR (Z _{AVG})	0,992	0,974	0,893	0,703
INLET VOLUME, (m ³ /h) (WET)	35890	10747	2314	767
DISCHARGE CONDITIONS				
PRESSURE (BarA)	107611	101614	104494	101020
TEMPERATURE (°C)	6,75	24,62	58,75	184,00
C _p /C _v (K ₂) OR (K _{AVG})	1714	188,5	132,0	163,5
COMPRESSIBILITY (Z ₂) OR (Z _{AVG})	1254	1271	1404	1655
	0,990	0,970	0,887	0,789

The high-pressure section delivers approximately 2683 psi (185 bar) with a molecular weight of 44. Therefore, the density is as high as 17.6 lb/ft³ (282 kg/m³). The same density for a natural gas compressor is achieved at a pressure of 8557 psi (590 bar).

The first impeller of the low-pressure section is typically a 3D wheel designed for high peripheral Mach number (flow coefficient of 0.088 and peripheral Mach number of 0.85). The overall pressure ratio of 103:1 will reduce the volumetric flow from 35889 to 357 m³/h. For this reason, there is a strong reduction in the overall flow path. This results in the impeller exit width reaching 0.275 in (7 mm) in the last stage and 0.078 in (2 mm) in the diffuser. The total absorbed power is roughly 17433 hp (13 MW). Special attention had to be given to the last section statoric components. In order to guarantee an

optimum flow into the first stage impeller, inlet volutes were designed to reduce loss coefficients and Mach number distortion over 360° degrees.

Figure 5 shows a loss coefficient comparison between a constant inlet plenum and the variable inlet plenum optimized for the Gorgon application (Figure 6).

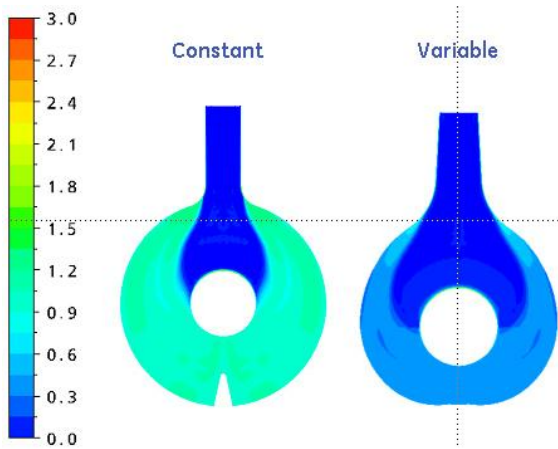


Figure 5. Loss coefficient CFD comparison between constant and variable inlet volute

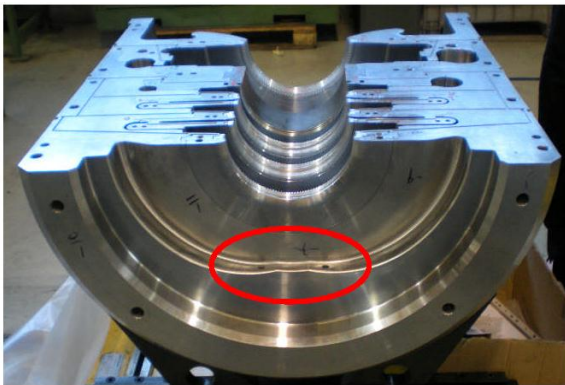


Figure 6. CO₂ Compressor diaphragms inlet volute – lower diaphragms (HP casing)

MATERIALS

Due to the presence of H₂S, CO₂ and water, corrosion resistant materials for both forged and casted components were used. The LP compressor (Figure 7) uses SA182F6NM for the casing and covers and forged statoric parts, 17-4PH for impellers, and CA6NM for casted diaphragms. The HP compressor (Figure 8) uses 17-4PH for casing, covers, diaphragms and impellers. The materials for the HP compressor are suitable for -130°F (-90 °C) minimum notch impact energy (NIE) to accept low temperatures resulting from depressurization.

Special welding procedures were qualified to comply with both NACE and minimum NIE requirements for the LP casing, using Inconel 276 as filler material. Note that because Inconel has different tensile properties from the base material, the final welded joint has mechanical characteristics lower than the base material. However, these values are well within the engineering design requirements.



Figure 7. LP compressor casing before hydraulic test



Figure 8. HP compressor casing during hydraulic test

ROTOR DYNAMIC DESIGN

The Fulton diagram (Figure 9) shows the criticality of the HP compressor. The operating point indicated on the map is beyond API617 limits but within the OEM safe limits.

The compressor is within the OEM acceptance range because of extensive experience with the same compressor types and applications.

The rotor is equipped with five impellers of 11.8 in (300 mm) size and is supported by journal bearings. A full stability level 2 analysis following API 617 7th edition was performed. The use of a Honeycomb (HC) seal on the balance piston plus swirl brakes (Figure 10) on all the impeller labyrinth eyes were required to meet stability criteria.

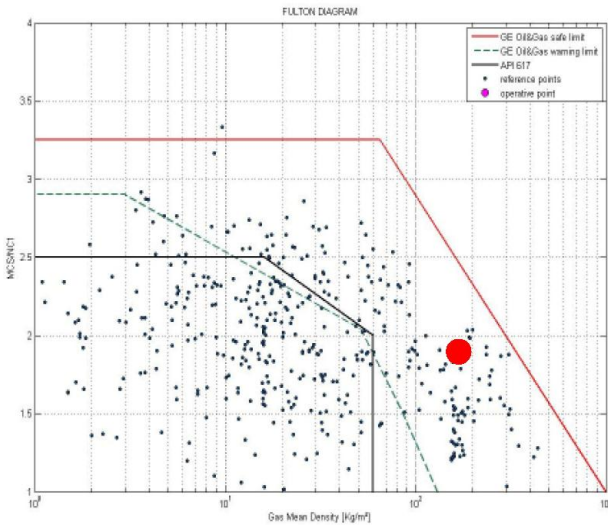


Figure 9. Fulton Diagram for HP casing

The use of FEA (Figure 11) for the bundle and rotor assembly was needed to optimize the HC tapering under running conditions.

The final calculated logarithmic decrement, including bearings and any destabilizing aerodynamic forces coming from the seals (impellers and balance drum), was found to be well beyond +0.2.

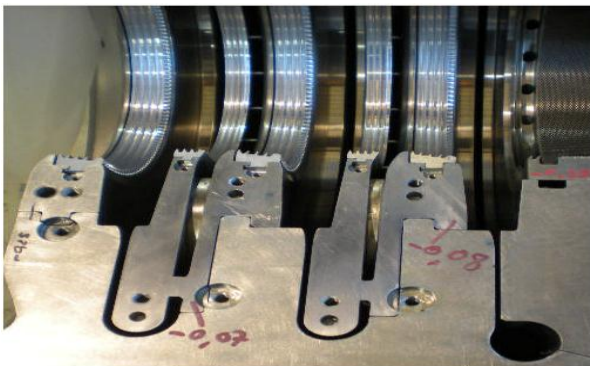


Figure 10. Swirl breaks and honeycomb

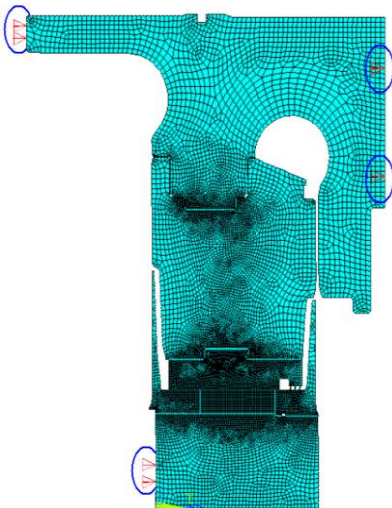


Figure 11. FEA analysis on exhaust volute

COMPARISON BETWEEN MECHANICAL TEST AND ANALYTICAL RESULTS

Both the LP and HP compressor casings were tested with excellent results in terms of vibration levels and critical speed location. This testing was conducted under a vacuum in accordance with API617 mechanical testing requirements (Figure 12).

Also the analytical modeling and predictability has been demonstrated during the unbalance shop test rotor response. The testing demonstrated very good correlation between the analytical predictions and the as tested results.

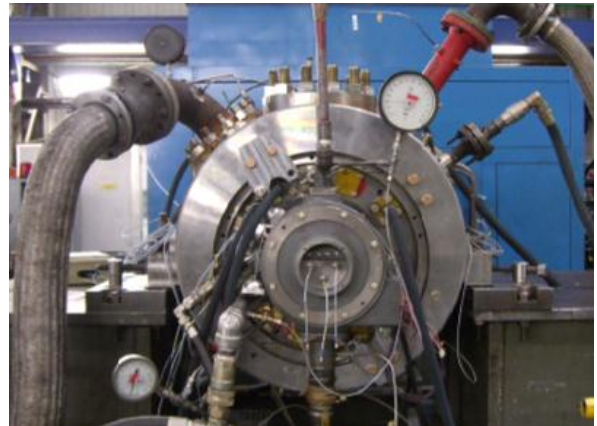


Figure 12. HP casing during MRT

Both HP and LP compressors results are presented in this article.

Figures 13 through 16 show the HP casing bearing radial probe bode plots recorded during mechanical run test (MRT), Table 2 provides the predicted critical speed values and relevant amplification factor (AF).

Figures 19 through 22 show the LP casing bearing radial probe bode plots recorded during mechanical run test (MRT), Table 3 provides the predicted critical speed values and relevant amplification factor (AF) for LP casing.

Comparison of predicted and measured values shows the following results:

HP Compressor Casing

- The measured critical speed around 6250 rpm that falls in between the predicted range 5900-6550 rpm;
- The max P-P vibration levels at MCS are below 0.62 mils (16 μm), resulting from the high level of balancing achieved with the high speed balancing
- The max AF calculated from the testing bode plots is 3.5, it is well within the predicted range 2.8 –5.7.

LP Compressor Casing

- The measured critical speed around 3000 rpm that falls in between the predicted range 2950-3000 rpm and very damped;
- The max P-P vibration levels at MCS are below 0.98 mils (25 μm)
- The max AF calculated from the testing bode plots is 3.5, it is below 5, well within the predicted range 6.23 –7.14.

Following API617 requirements and to validate HP and LP casings analytical model, an unbalance shop verification test has been performed.

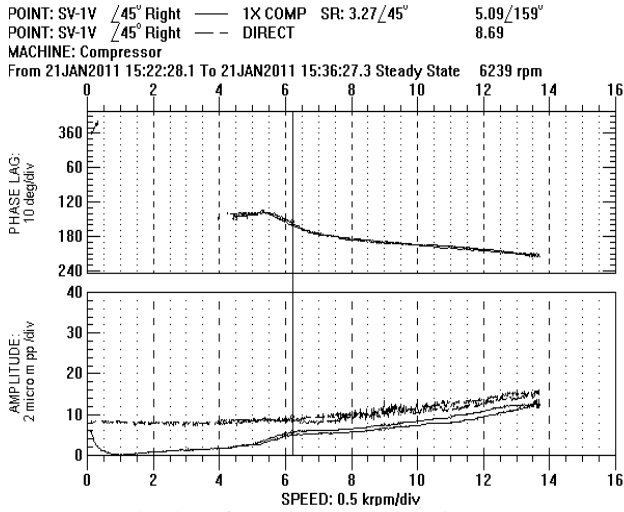


Figure 13. Bode plot of Bearing 1, X direction. HP compressor casing

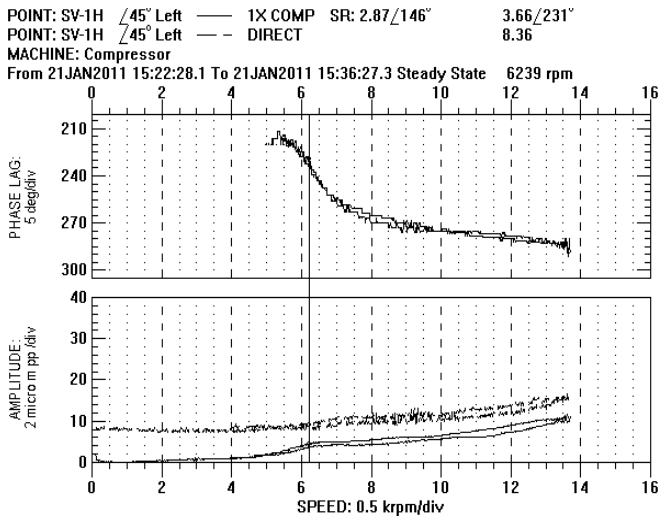


Figure 14. Bode plot of Bearing 1, Y direction. HP compressor casing

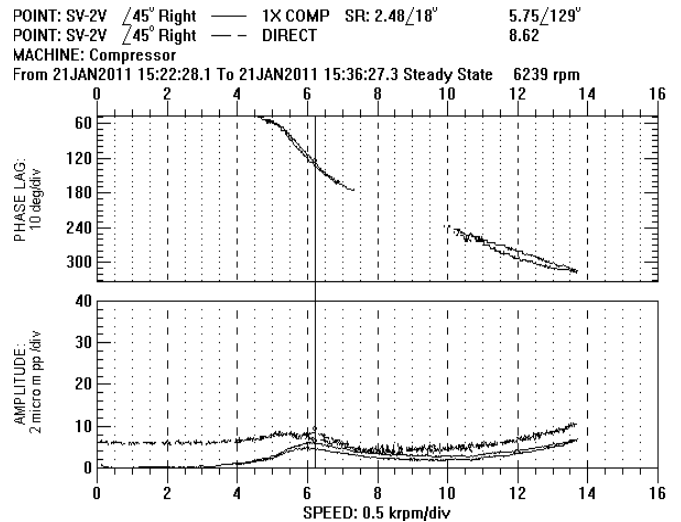


Figure 15. Bode plot of Bearing 2, X direction. HP compressor casing

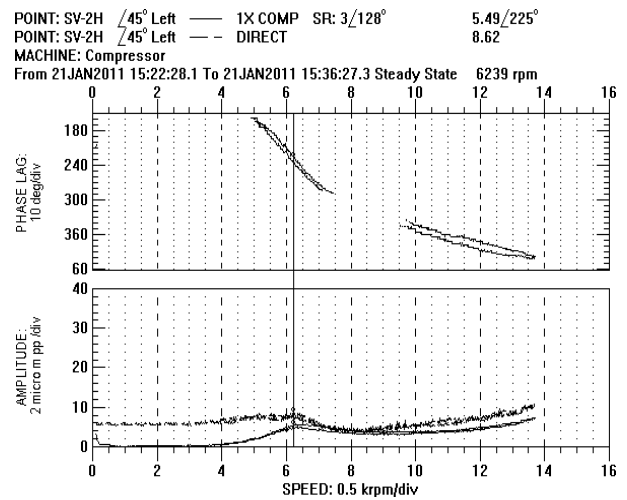


Figure 16. Bode plot of Bearing 2, Y direction. HP compressor casing

Table 2. Calculated critical speeds and relevant AF. HP compressor casing

1 ST CRITICAL SPEED				
Supports stiffness	Frequency (CPM)	Amplification factor	Separation margin ACTUAL (%)	Separation margin REQUIRED (%)
MINIMUM	5900	2.76	43.35	3.55
MAXIMUM	6550	5.66	37.10	12.91

2 ND CRITICAL SPEED				
Supports stiffness	Frequency (CPM)	Amplification factor	Separation margin ACTUAL (%)	Separation margin REQUIRED (%)
MINIMUM	17200	1.57	25.82	Not Required
MAXIMUM	25150	32.62	83.98	26.45

Vibration measured data during MRT and unbalance shop verification test values have been post-processed to obtain the P-P vibration levels due solely to the applied unbalance weight (465g.mm).

The unbalanced weight installed on shop test shaft drive end (Figure 17) was calculated in advance, as required by API617 for the lateral rotordynamic reports.



Figure 17. Weight installed on shop test coupling

Post-processing analysis consists of vectorial subtraction between mechanical run and unbalance response test vibration levels at each test speed (rpm). Figure 18 shows extremely very good correlation of the predicted versus measured values. The unbalance rotor response at any speed always remains between the predicted curves.

These results verify the compressor rotordynamic analytical model. In particular this is confirmed by the fact that at MCS, the measured value of 0.59 mils P-P (15 μm P-P) falls in between the predicted range 0.472-0.98 mils (12 - 25 μm) for HP compressor. For LP compressor, the Figure 18 shows a good matching of the predicted values versus the measured ones, being the rotor response under unbalance weight influence very close to the predicted curves (0.118 mils of gap @ MCS) while there is a perfect overlap crossing the critical speed.

It needs to be highlighted that lateral analysis is performed assuming no influences from the compressor seals including the honeycomb seals.

The MRT performed under a vacuum simulates the lateral analysis conditions and the test results have validated the lateral analytical model, with similar seal conditions.

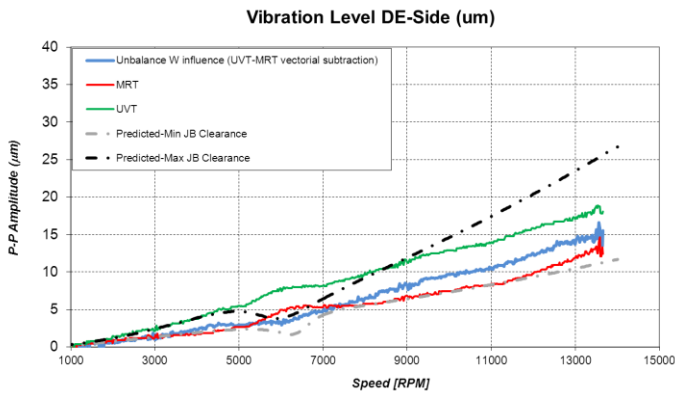


Figure 18. Predicted and tested rotor response comparison for HP compressor

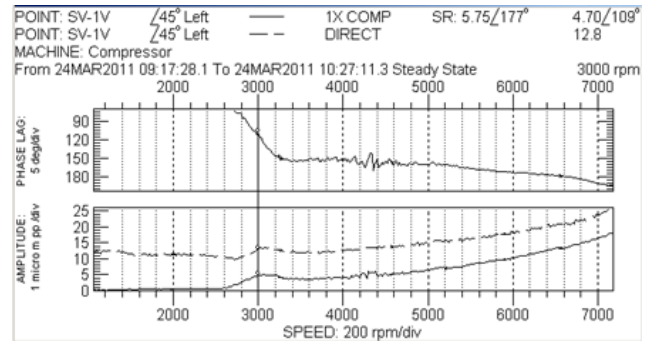


Figure 19. Bode plot of Bearing 1, X direction. LP compressor casing

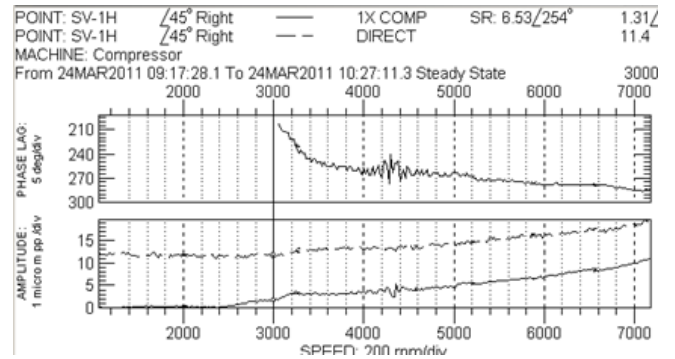


Figure 20. Bode plot of Bearing 1, Y direction. LP compressor casing

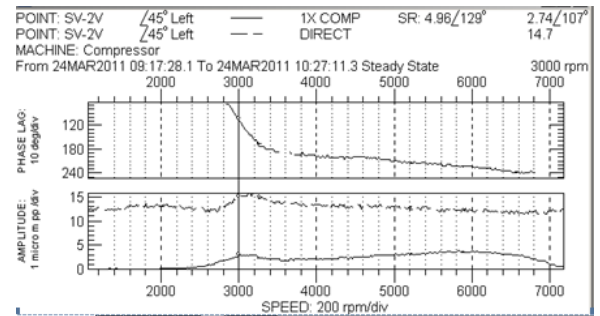


Figure 21. Bode plot of Bearing 2, X direction. LP compressor casing

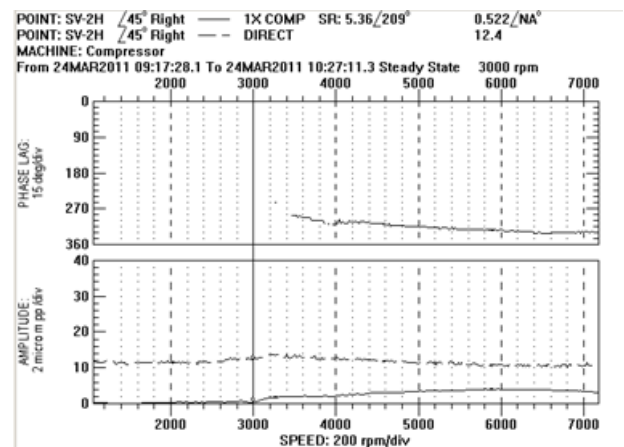


Figure 22. Bode plot of Bearing 2, Y direction. LP compressor casing

Table 3. Calculated critical speeds and relevant AF. LP compressor casing

1 ST CRITICAL SPEED				
Supports stiffness	Frequency (CPM)	Amplification factor	Separation margin ACTUAL (%)	Separation margin REQUIRED (%)
MINIMUM	2950	6.23	40.67	13.41
MAXIMUM	3000	7.14	39.67	13.96

2 ND CRITICAL SPEED				
Supports stiffness	Frequency (CPM)	Amplification factor	Separation margin ACTUAL (%)	Separation margin REQUIRED (%)
MINIMUM	8100	2.50	24.1	10.05
MAXIMUM	9400	3.07	44.02	16.23

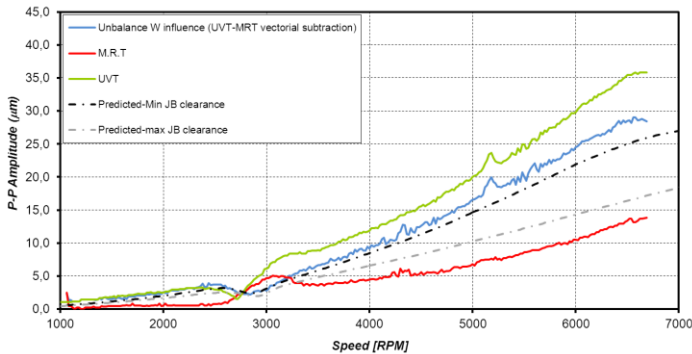


Figure 23. Predicted and tested rotor response comparison for LP compressor

COMPRESSOR PACKAGE CONFIGURATION, MAINTENANCE REQUIREMENTS AND HUMAN-FACTOR ASPECTS

Design requirements for the Gorgon Project require OEMs to maximize the modularization of equipment including the compressor trains (Figure 24). This results in the need to optimize the package overall dimensions to respect very stringent space constraints and ensure maintenance access is provided.

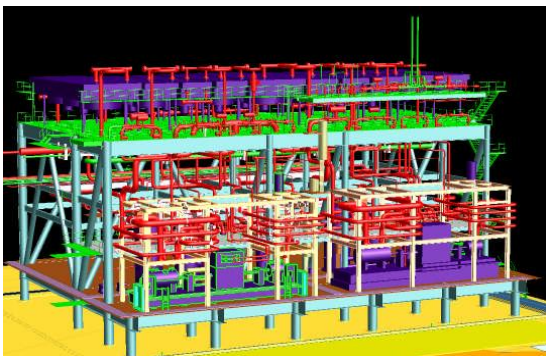


Figure 24. CO₂ Compression Modules layout

Modularization and compressor bundles maintenance constraints have been a major driver for final compressor train arrangement. The axial split casing originally selected for the LP casing (Figure 25) did not allow for easy bundle removal with top mounted nozzles. Consequently the design was modified, changing the motor driver from single shaft end to a

double shaft ended design (Figure 26).

The resulting configuration allows for bundle removal (Figure 27) without disassembly of the process piping since the compressors are located at each end of the compressor string.

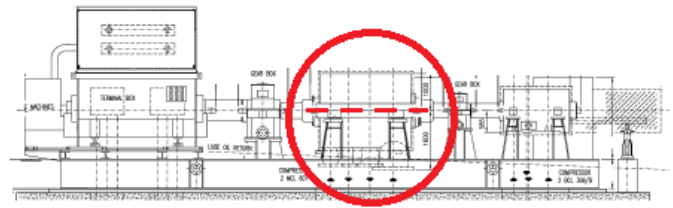


Figure 25. Original configuration – Single end motor shaft with LP axial split casing, HP barrel compressor type

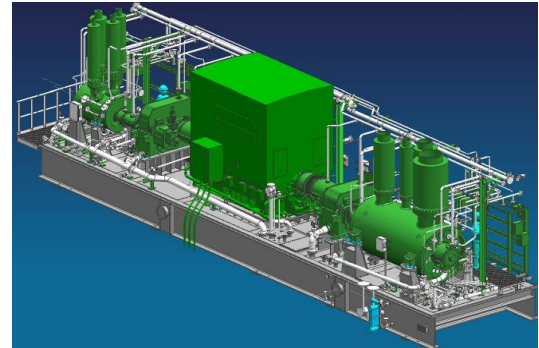


Figure 26. Final configuration – Double end motor shaft with HP and LP barrel compressors type



Figure 27. HP bundle removal after MRT

The project engineering challenges include: ergonomic design requirements, ease of maintenance requirements, compressor supports stiffness analysis for installation on module steel work, and operability assessment. To facilitate the package design, a 3D model review was conducted to meet the project requirements for minimum access and clearances for maintenance. 3D model as a design tool during detail engineering phase allowed for significant improvement in terms of maintenance and access to the package.

DRIVER TECHNOLOGY

During the design phase, a study was performed between voltage source inverters (Figure 28) and 12-pulse PWM

inverters (Figure 29). Voltage source technology was definitely applied on the project. This technology is able to decrease stresses that can limit the life of the equipment by gradually increasing power to accelerate the train to full speed. The VFD can provide full rated torque during acceleration from zero speed and eliminates current inrush into the motor.

Project VFD meets the most stringent harmonic requirements for voltage and current distortion. By minimizing voltage and current distortion, the VFD protects other on-line equipment from harmonic disturbances. This eliminates the need for costly and inefficient harmonic filters and eliminates associated resonance problems. It also eliminates significant drive induced torque pulsation including pulsations at low speeds and avoids the need for specialized expensive flexible couplings.

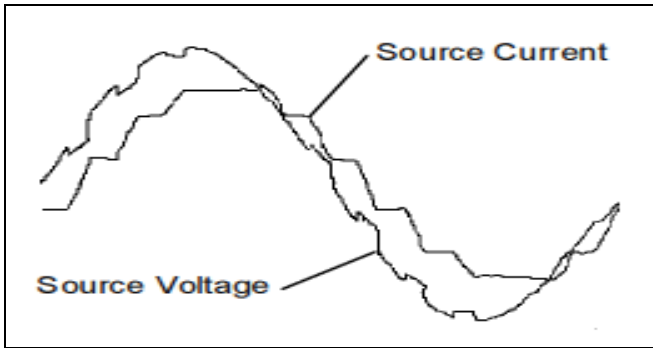


Figure 28. Typical 12 pulse input waveform

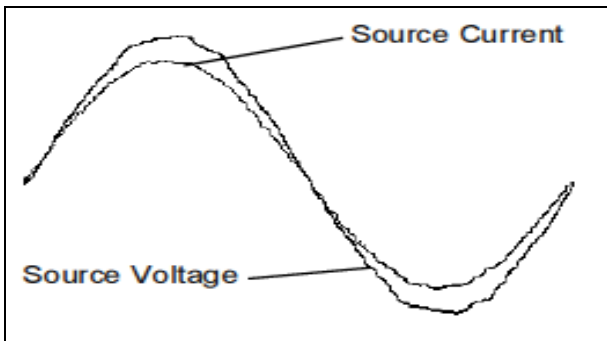


Figure 29. Typical input waveform of voltage source technology.

SHAFT LINE CONFIGURATION AND TORSIONAL ANALYSIS

The compressor train consists of a motor with a double-ended shaft configuration. Each end of the motor drives a speed-increasing gearbox that drives the two compressor bodies. This complex configuration, combined with the VFD capability, required extensive lateral analysis of each machine and torsional analysis of the overall train.

If a torsional vibration frequency matches a resonance frequency, large torsional deflections and internal stresses can be generated. Continuous operation under these conditions could result in fatigue failure of system components. A free-vibration analysis and forced-response analysis were conducted to complete the analytical review including rotor response to static and harmonic torsional loads.

VFD motors generate pulsating torques. Even though the pulsating torques from a voltage source VFD are very small, with respect to the main torque, they can excite compressor train resonances with potential damage to shafts and/or couplings.

The first step of the torsional analysis was to define the equivalent torsional shaft, starting from the real rotor configuration (Figure 30).

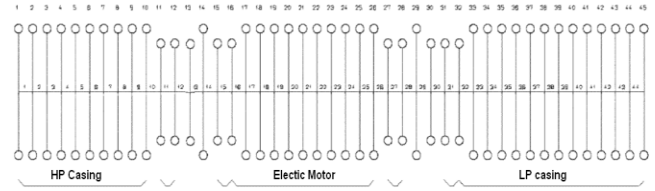


Figure 30. Shaft line model

In the second step, an analytical study of the equivalent system was performed, allowing the calculation of natural frequencies and the relevant mode shapes. The most important results have been summarized in the Campbell diagram (Figure 31)

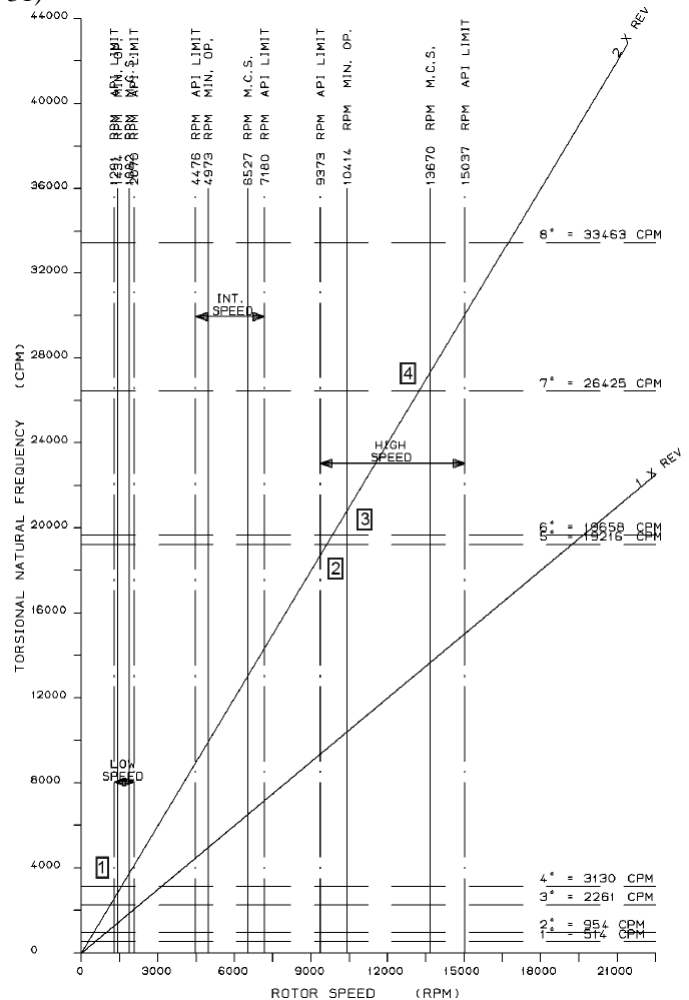


Figure 31. Campbell diagram

In the third step, where the API-617 safety margins could not be met due to design reasons, a stress analysis was performed.

The results were considered acceptable if the maximum shear stress (zero to peak) was lower than 4% of the ultimate tensile strength of the material. The criterion of 4%, used as standard by the OEM, was derived from NAVY Mil. std.167. The acceptance criteria consider very restrictive values of the stress concentration factors and it is in accordance with the acceptance criteria in literature.

The stress analysis performed is quite conservative, although it permits a quick evaluation of the fatigue stresses. In the case the results do not satisfy the limits established by the criterion mentioned above, a more classical fatigue evaluation is performed (Figure 32).

Finally, in the fourth step, the torques due to electrical faults, acting on train components, are calculated (See Figure 33). The electrical faults include: three phase short circuit, line to line short circuits, and out of phase synchronization.

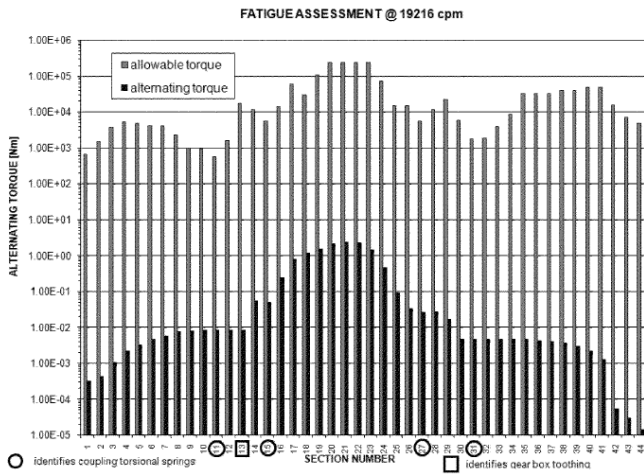


Figure 32. Fatigue evaluation

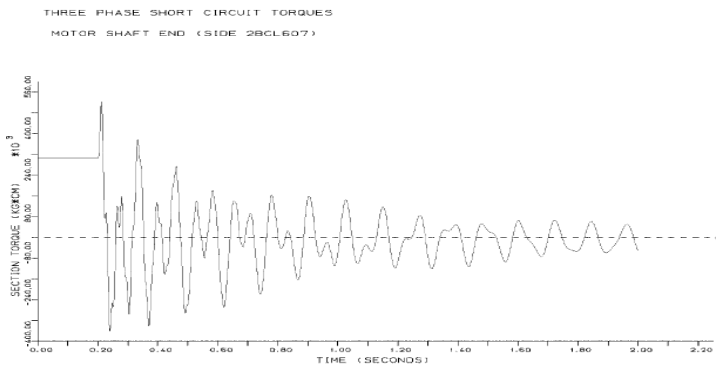


Figure 33. Three phase short circuit torques

The damped torsional system is represented by a reasonable number of lumped inertias, connected by massless torsional springs, and including speed-dependent damping. For torsional systems, the damping is usually very low and does not significantly influence the torsional modes. For the purposes of calculating natural frequencies and mode shapes, the effects of damping within the system may be neglected.

The torsional system Equation (1) is:

$$J \cdot \ddot{\Theta} + C \cdot \dot{\Theta} + K \cdot \Theta = M \quad (1)$$

To determine the natural frequencies the damping can be neglected and the moment is zero, Equation (2) is generated:

$$J \cdot \ddot{\Theta} + K \cdot \Theta = 0 \quad (2)$$

The natural frequencies are the eigenvalue of the above Equation (3), so:

$$\det(-\omega^2 \cdot J + K) = 0 \quad (3)$$

where ω is the generic eigenvalue, Ω is the eigenvalue matrix (diagonal, n by n, [1/s]) and contains the natural frequencies of the system.

The results of the overall train analysis are that there are no intersections between the torsional natural frequencies and the possible exciting sources of one and two times rotational speed. Since the motor is a VFD, a motor torque ripple (Figure 34) excitation analysis was conducted for the different operating conditions. The analysis shows that the expected torque ripple is extremely low.

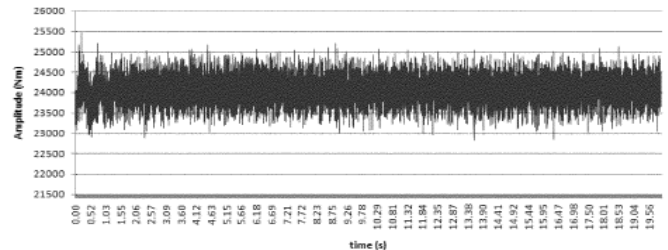


Figure 34. VFD Torque ripple sample time

Torsional train behavior and VFD torque ripple will be validated through an extensive test campaign. The test campaign will be conducted with the machine fully assembled in a string test configuration.

Testing will be conducted during steady state and transient conditions (start-up) by means of OEM dedicated measurements devices installed on the couplings. Frequency analysis will be conducted with data acquired during the string testing, waterfall (Figure 35) technique will be extensively applied to validate torsional behavior and torque ripple levels.

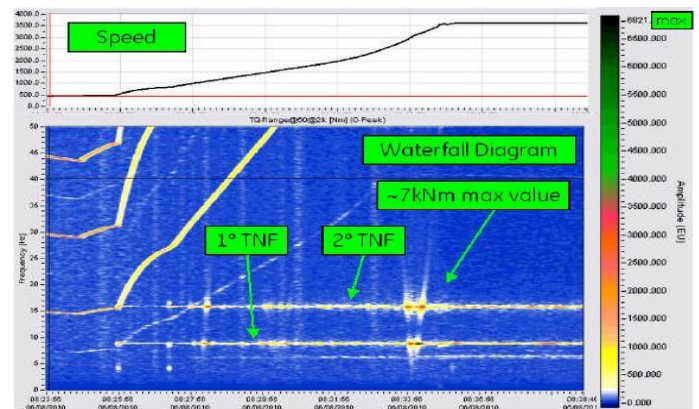


Figure 35. Waterfall analysis

DRY GAS SEALS AND SYSTEM PHILOSOPHY

Labyrinth seals are extensively applied in CO₂ compressor applications. However the need to reduce fugitive emissions requires the use of DGS instead of traditional labyrinth seals. John Crane T82XP tandem DGS, with N₂ intermediate injection and labyrinth barrier seal have been selected (See Figure 36).

All relevant auxiliaries and panels have been designed for control and sealing protection purposes. N₂ intermediate injection is provided to avoid any release of process gas into the secondary atmospheric vent. DGS materials selection was based on NACE MR-01-75 requirements.

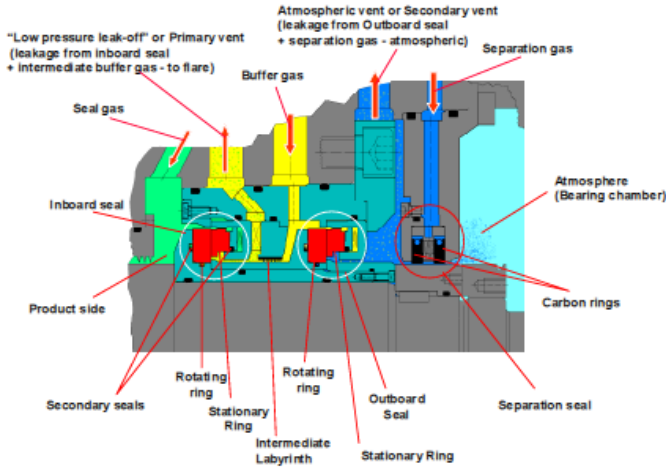


Figure 36. Typical tandem DGS layout with N₂ intermediate injection

The DGS system is composed of two pressure levels supporting the LP and HP casings, with no external buffer available during transient operations.

During commissioning, the compressor will be operated on N₂ to prove out the compressor and associated systems prior to operating on CO₂. Operation of the compressor with N₂ was one of the operating conditions considered for the DGS design.

In order to eliminate any potential risk of condensate formation and for compliance with API617, a gas heating system has been installed for each seal pressure level. The heaters maintain gas temperature a minimum of 68°F (20°C) above the dew line of the process gas at all times.

An external seal gas source is not available at the conditions required for this application. To protect the compressor seals during transient operating conditions and to ensure the correct seal gas flow, even during standstill and critical transients, a dedicated seal gas booster system (See Figure 37) has been utilized. This system is based on a seal-less reciprocating compressor that does not allow any contact of the sealing gas with the external environment.



Figure 37. Seal gas booster skid

During standstill conditions, the use of seal gas from the compressor discharge is not possible and the DGS is at risk of contamination especially by heavy hydrocarbon condensation. Normally to mitigate this risk, the compressor would be depressurized after a trip. The installation of the seal gas boosters allows the compressor to be kept pressurized after a trip, while the DGS remains correctly buffered and ready to be restarted, with the heater working (see Figure 38). This design avoids the need to depressurize the compressor during process trips. All the seal gas support system components have been modularized on two separate skids, for the LP and HP casings.

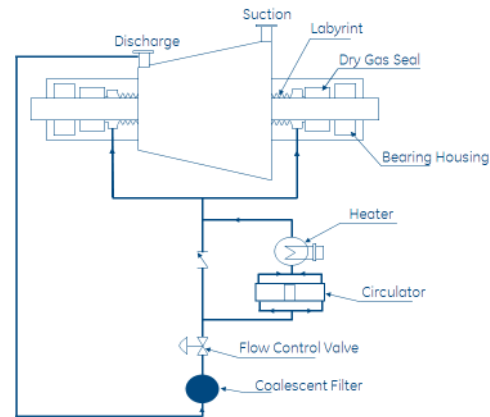


Figure 38. Booster simplified schematic diagram

Very high discharge temperatures generated from the CO₂ compressor (above 428°F (220°C)) LP casing, required special design for the secondary sealing elements for the DGS.

During normal operation, auto-buffer is provided by the 3rd section (see Figure 39) for LP and HP casings. Booster and heaters are always on during transient conditions (start-up and shut-down) until seal gas is established from the 3rd stage discharge (auto-buffering).

Depending on operating conditions, the heater could be activated in order to ensure the process gas temperature is above 266°F (130°C) to avoid sulfur condensation.

Dedicated controls were developed for the seal systems taking into consideration LP and HP pressure levels and temperature control.

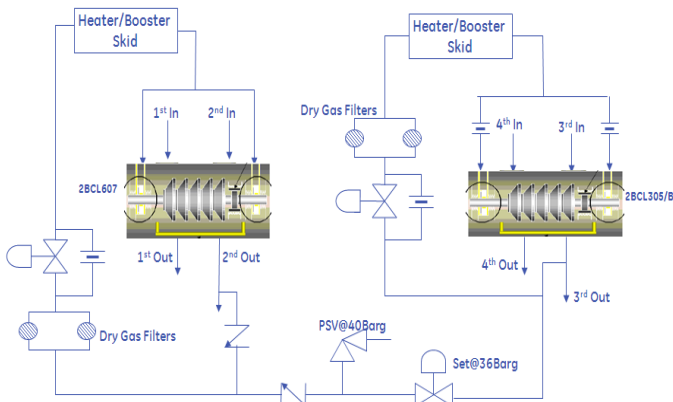


Figure 39. DGS System simplified schematic diagram



Figure 41. HP compressor casing instrumented as per ASME PTC10 requirements.

STRING TESTING ACTIVITIES

An intensive testing campaign to validate string mechanical behavior and compressors thermodynamic performance of all machines has been successfully conducted during June -2011, in Massa (Italy) testing facility.

The testing scope included following activities:

- ASME PTC-10 Type 1 test on LP and HP casings. Compressor curves at 90% and guaranteed curves were explored from surge to overflow, 5 test points for each curve
- Full speed, Full Load, Full Pressure complete string test
- Pulsating torque validation

In order to validate as much as possible the compressor performances, compressor operating envelop has been investigated running machine at 90% and at 105%.

4 hours running Full Speed Full Load Full Pressure test was conducted with 100% CO₂, matching the compressor full power of 17030 hp (12.7 MW), at maximum continuous speed, and 3290 psi (200 Bar) delivery pressure.

Complete testing gas loop (see Figure 40) has been designed and assembled to support all testing requirements. The test loop included additional instruments (see Figure 41) needed to satisfy all ASME PTC-10 Type 1 code requirements in terms of instrument quantity and accuracy.

A dedicated stress analysis was conducted for the test loop to validate maximum stress on compressor nozzles and the test loop process piping including support locations. Contract components including lube oil systems, VFD and all dry gas seal system equipment have been used.



Figure 40. CO₂ Test bench and gas loop (Massa, Italy)

STRING TESTING RESULTS

ASME PTC10 Performance Test Results

As required by ASME PTC10, once the test is completed under similitude conditions and to assess the train performance, two main analyses have been carried out by superimposing the predicted curves with the revised ones (as calculated after the tests):

- Stage by stages performance comparison (Figure 42-45);
- Overall train outlet pressure and power comparison (Figure 46-47).

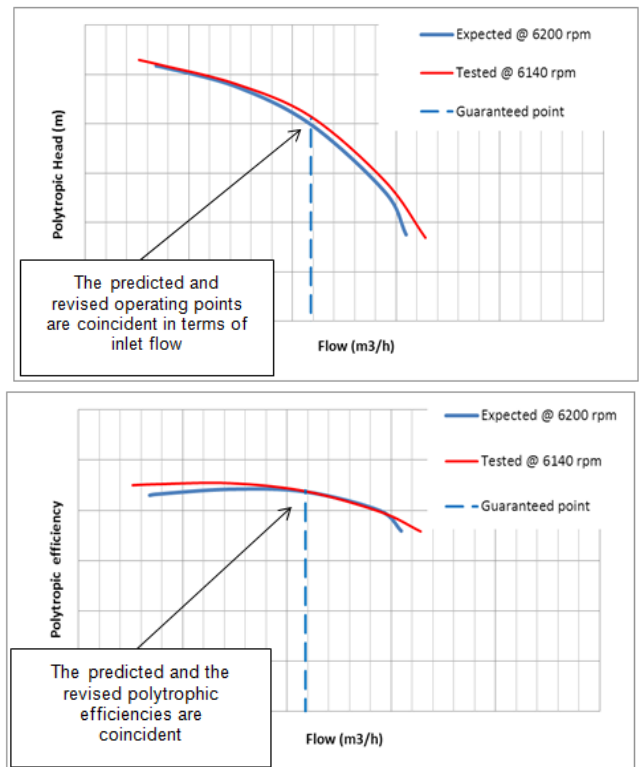


Figure 42. 1st stage LP compressor ASME PTC10 Type 1 test results

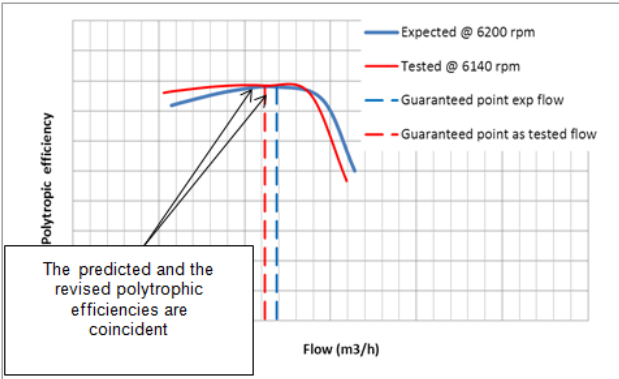
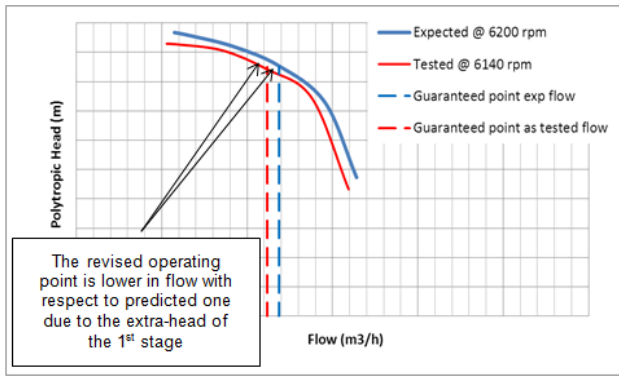


Figure 43. 2nd stage LP compressor ASME PTC10 Type 1 test results

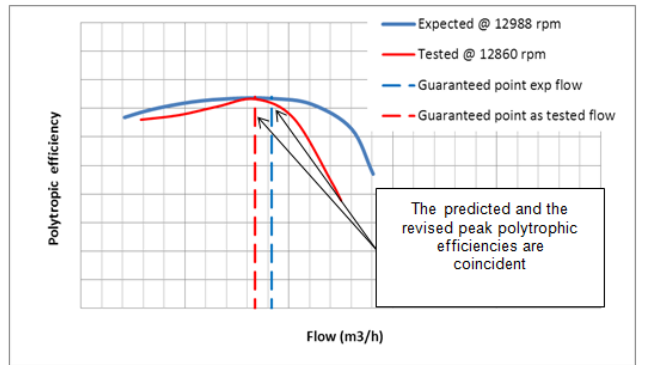
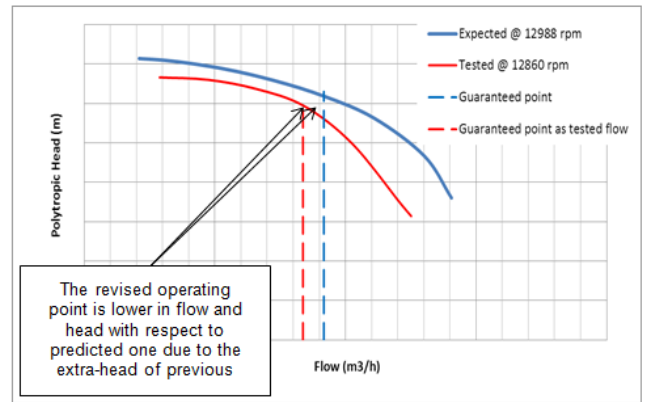


Figure 45. 4th stage HP compressor ASME PTC10 Type 1 test results

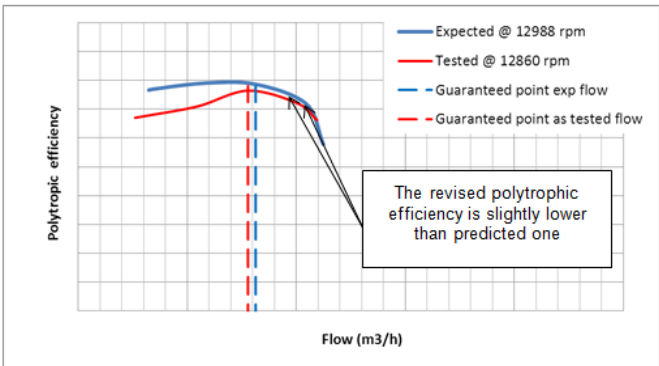
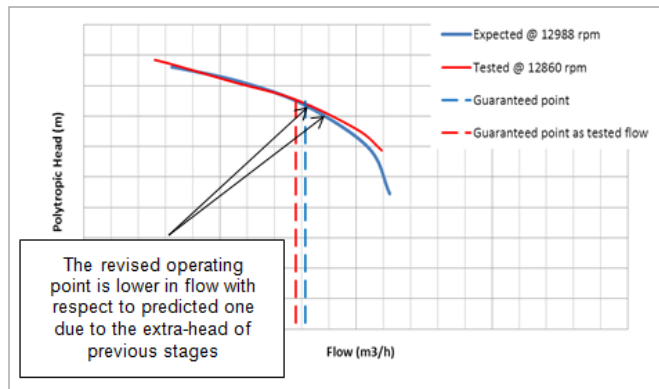


Figure 44. 3rd stage HP compressor ASME PTC10 Type 1 test results

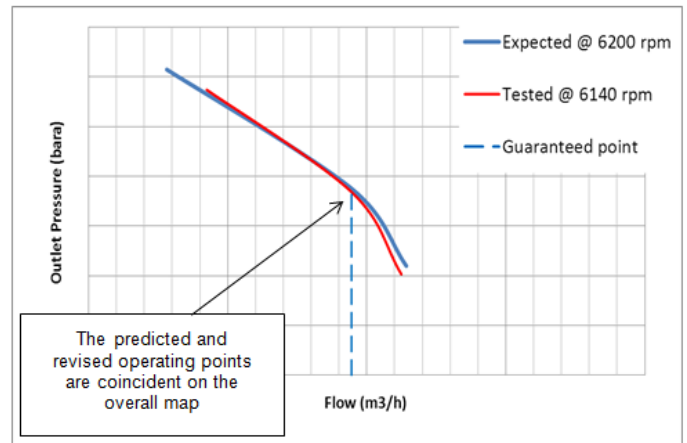


Figure 46. Overall performance curve, discharge pressure

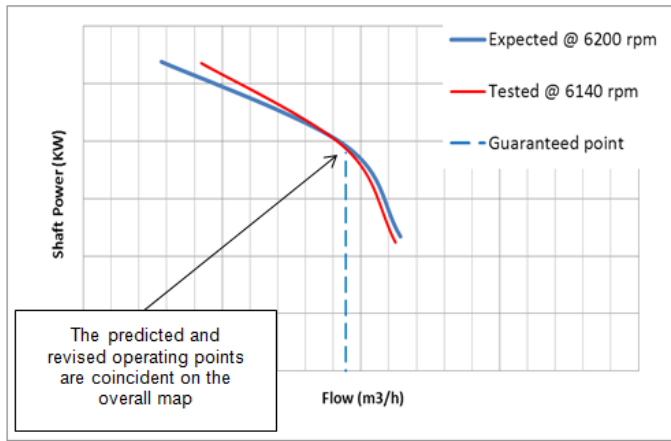


Figure 47. Overall performance curve, absorbed power

The first three stages show extra-head and polytrophic efficiency in line with expected values on the guaranteed point, while the 4th stage results in head lower than expected as well as left and right curve limits and polytrophic efficiency in line with the guaranteed value. Overall is observed a contraction of the 4th stage envelope likely due to the high Mu condition (above 0.9) of the 1st impeller of this section.

However the extra-head of the first 3 stages produces two beneficial effects on the overall performance of the train:

1. The guaranteed operating conditions can be met reducing the driver speed. The Table 4 presents a summary of the four stages in terms of outlet pressures, gas power and speeds comparing the expected and revised figures.
2. The inlet flow of the 2nd, 3rd and 4th stages are reduced as highlighted in the Figures 42-45 by the dashed vertical lines. Hence the extra-head of the first 3 stages produces a beneficial effect on the 4th stage inlet flow that is recalibrated on its own peak efficiency maintaining the left and right side margins very close to the expected values. The Table 5 shows a comparison of the turndown and choking margins for all the different operating points.

Table 4. Comparison of expected and As-Tested results

	1	2	3	4
OUTLET PRESSURES (bara)				
Exp	6,75	24,62	58,75	184
As Tested	6,90	24,94	60,36	184
GAS POWER(kW)				
Exp	3383	3826	1995	2635
As Tested	3428	3778	2057	2555
ROTATING SPEED (rpm)				
Exp	6201	6201	12988	12988
As Tested	6140	6140	12860	12860

Total Exp Gas Power=11839 kW
 Total as Tested Gas Power=11818 kW (-0.2%) @ -1% vs. exp speed

Table 5. Comparison of Turn-Down and Chocking margins

PREDICTED		1° Stage		2° Stage		3° stage		4° Stage	
CASE	turndown (%)	choking (%)							
GUARANTEED	28	113	29	117	27	113	41	125	
OP1	12	132	14	137	12	134	28	147	
OP2	25	117	27	120	25	117	39	129	
OP3	29	113	31	116	31	110	49	113	
OP4	27	113	28	119	22	118	33	140	
OP5	14	131	16	135	12	133	29	145	
OP6	16	127	22	127	27	117	26	150	
REVISED		1° Stage		2° Stage		3° stage		4° Stage	
CASE	turndown (%)	choking (%)							
GUARANTEED	29	115	27	118	28	114	38	122	
OP1	11	137	12	139	14	133	25	143	
OP2	25	120	25	122	26	116	35	126	
OP3	29	115	29	131	31	111	45	113	
OP4	29	116	26	120	24	118	29	135	
OP5	12	135	13	136	14	132	26	140	
OP6	15	132	17	132	25	120	19	148	

From testing results, the operability of the train has not been affected since the map extension, (relative to the revised inlet flows) remains practically the same of the predicted ones (only few percentages of variation for all the operating points) as well as the power and speed margins gaining in train flexibility (guaranteed point met with -1% speed). In addition the 3rd stage discharge pressure is kept in the range for maximum water removal never exceeding the limit of 65 bara to avoid CO2 dew point.

Finally, looking at the overall curves, it may raise a concern being the revised curve shorter on the left, in the area of the high pressure. In reality this is not a real concern since the 4th stage discharge pressure is limited at 3669 psi (253 bar) by a PSV and the difference between the revised and predicted curves appears well above this value.

Torsional Assessment and Pulsating Torque measurements

During start-up, four hours running at full-speed, full-power, full-pressure, and shut-down, torsional vibration of the train have been continuously measured and recorded.

By means of an OEM dedicated system installed on each coupling (see Figure 48), it was computed the angular velocity oscillation signal, about the average rotational speed of the machine: this was then converted into angular vibration signal using integration function (see Figure 49).



Figure 48. Torsional measurement system

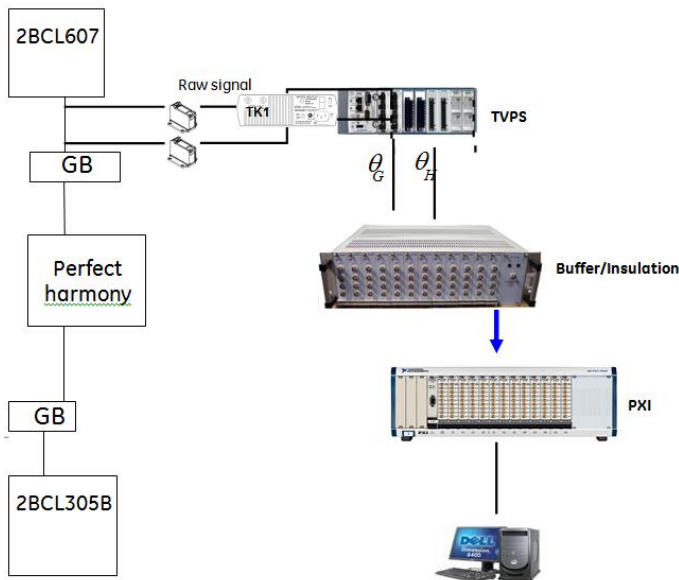


Figure 49. Load couplings instrumented during String test

This methodology, being rugged and reliable, allows to accurately evaluating torsional stress amplitudes in different machine sections and is suitable for a very wide range of test conditions.

The alternating torque has been calculated for each coupling by multiply the measured angular differential vibration with the spacer design stiffness, Equation (4):

$$C_{alt} = G \cdot (\theta_G - \theta_H) [N \cdot m] \quad (4)$$

Test results have confirmed very good predictability of torsional model used during design phase and negligible alternating torque respect to the coupling maximum allowable value (Table 6).

Comparison between test alternating torques (Table 7), measured on each coupling during all phases, and couplings max allowable values (Table 8) demonstrates that alternating torque generates by VFD are negligible: this reflects into an excellent overall train mechanical behavior and no risk of potential coupling failure.

	Torque Vibration HP high speed coupling [Nm]	Torque Vibration HP load coupling [Nm]	Torque Vibration LP load coupling [Nm]	Torque Vibration LP high speed coupling [Nm]
	1695	18077	18077	8474

Table 6. Load Coupling design max allowable alternating torque

Table 7. Alternating torque measured during Full Speed Full Load Full Pressure, at steady state conditions

	Torque Vibration [2BCL305 - H5GB]				Torque Vibration [H5GB - EM]				Torque Vibration [EM - L5GB]				Torque Vibration [L5GB - 2BCL607]			
	1TNF	2TNF	3TNF	4TNF	1TNF	2TNF	3TNF	4TNF	1TNF	2TNF	3TNF	4TNF	1TNF	2TNF	3TNF	4TNF
MAX [Nm]	34	40	28	41	825	340	124	133	110	201	122	146	286	91	59	26
Average [Nm]	9.9	13	6.5	18	268	133	29	26	356	79	33	23	92	36	25	9.3

Waterfall (Figure 50) methodology has been applied to measure the real first four train torsional frequencies (Figures

51-54) and to compare with theoretical values indicated by torsional analysis conducted during design phase.

Results have shown a very good agreement between theoretical and measure torsional natural frequencies (Table 8), especially for the 1st, 2nd and 4th mode. The 4th mode is extremely damped, dedicated post processing was needed to distinguish the 4th mode from signal overall noise.

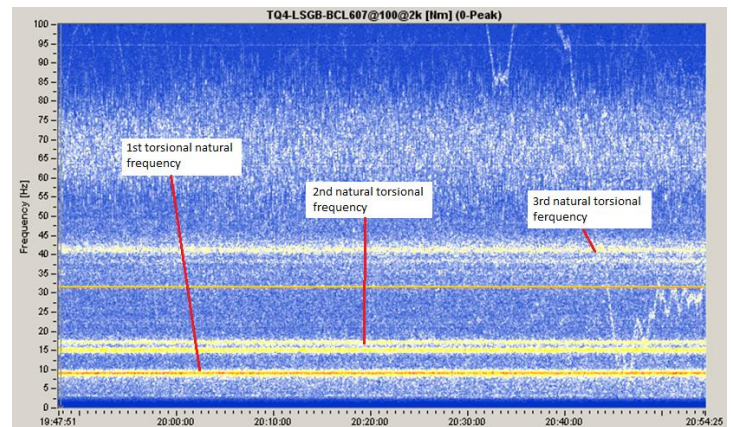


Figure 50. Waterfall showing measured natural torsional frequencies during String Test

Table 8. Torsional assessment resuming table

Torsional Frequency	1 st Mode	2 nd Mode	3 rd Mode	4 th Mode
OEM Theoretical (Hz)	8.6	15.9	37.7	52.2
OEM Measured (Hz)	9.2	17	41.3	53.0
3 rd Party Theoretical (Hz)	8.5	15.88	38.67	52.55

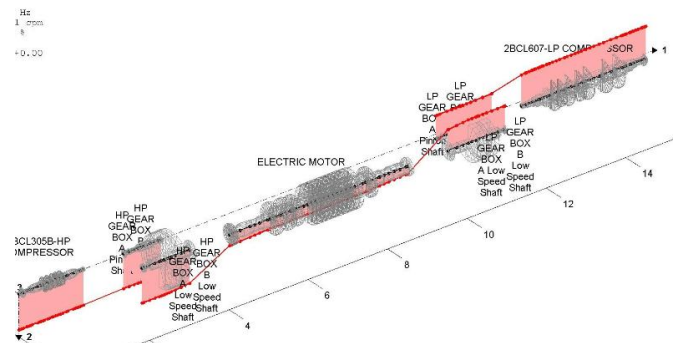


Figure 51. 1st torsional natural frequency

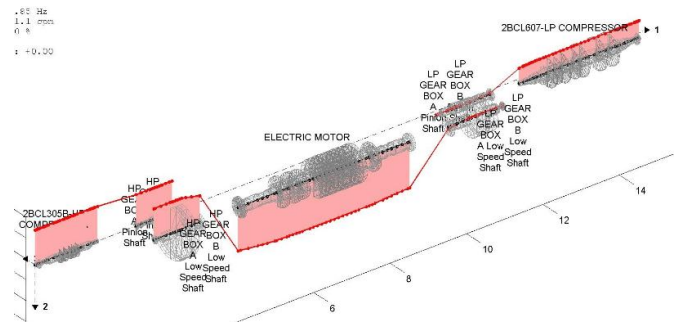


Figure 52. 2nd torsional natural frequency

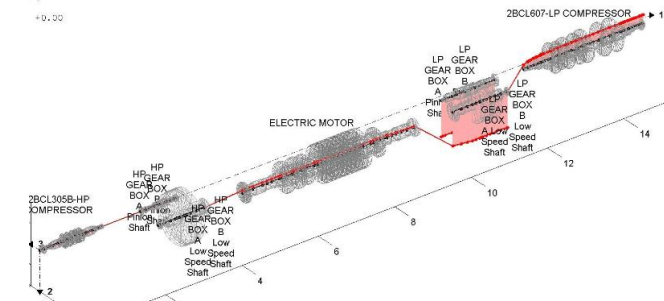


Figure 53. 3rd torsional natural frequency

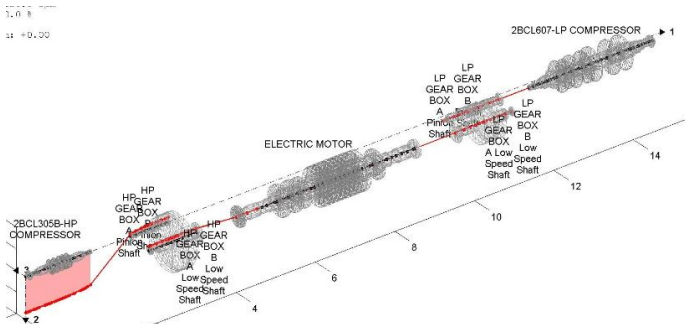


Figure 54. 4th torsional natural frequency

String Test mechanical test results

Main scope of Full Speed Full Load Full Pressure, conducted at maximum continuous speed and with final delivery pressure constantly at 2900 psig (200 Barg), was validation of complete unit overall mechanical behavior in terms of vibration and bearing temperatures.

Results have been extremely positive under all aspects, with extremely low levels of vibration for all rotating equipments : VFD motor, HP Gear Box, HP Compressor, LP Gear Box and LP Compressor.

Here below test results (Figures 55-58) of vibration radial probes of HP compressor, spectrums have been measured during ASME PTC10, at surge condition, 3118 psig (215 Barg) of final delivery pressure.

Direct maximum vibration level measured has been 0.75 mils P-P (19 microns P-P) on HP casing, 0.98 mils P-P (25 microns P-P) on LP one .

During each test phase, very low vibration amplitudes of both synchronous and sub-synchronous part have been recorded. On the HP compressor the honeycomb seal on the stage division wall was acting as real third bearing set in the middle of the rotor. The damping and the stiffness provided by that type of seal resulted in two beneficial effects on the rotor dynamic of the HP compressor:

1. Limiting the P-P vibration amplitude at very low levels in the whole speed range;
2. Increasing the first natural frequency of the rotor and relevant damping, hence providing very stable operation till the surge margin at MCS.

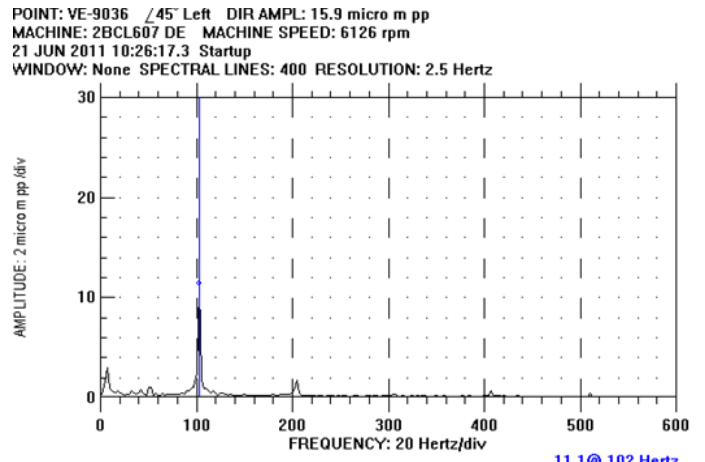


Figure 55. 1st stage LP compressor drive end side, at surge

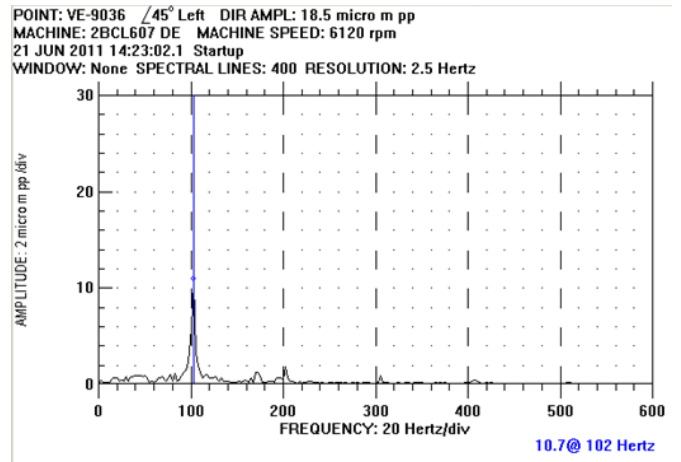


Figure 56. 2nd stage LP compressor drive end side, at surge

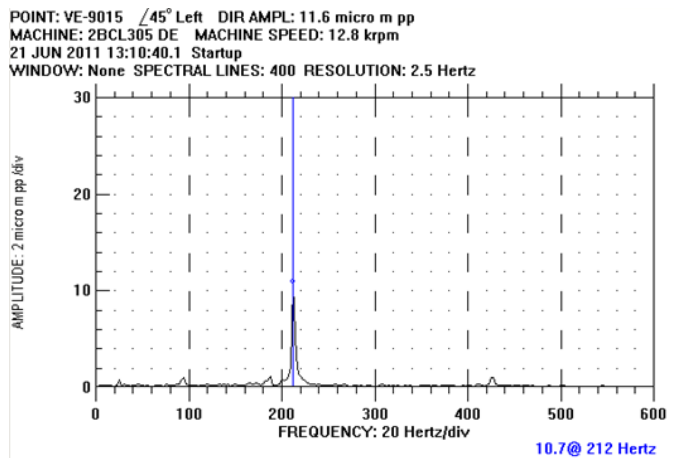


Figure 57. 3rd stage HP compressor drive end side, at surge

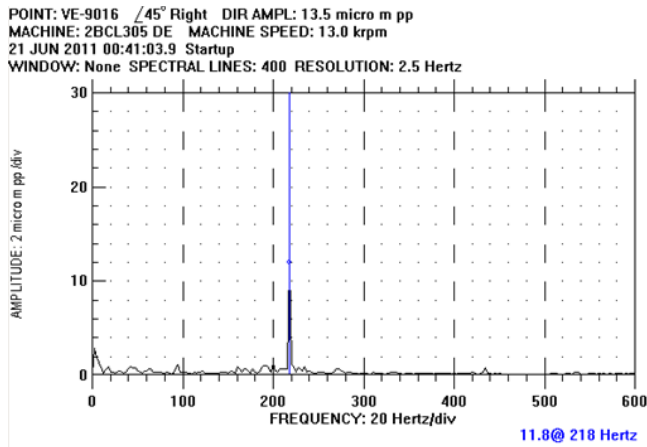


Figure 58. 4th stage HP compressor drive end side, at surge

One of main peculiarities of the package is the double end motor shaft, the motor is between the two load-increasing gear boxes. This aspect has been deeply investigated during design phase, especially for what concerns any potential lateral-torsional interaction that could be generated on the gear-box mesh, with consequent risk of high vibration.

Simulations were conducted applying on the motor core the waveform (function in Nm vs time in s) of pulsating torque components, in order to investigate the responses in terms of lateral displacements in correspondence of gear boxes 8 bearings locations.

The dynamic model (Figures 59-61) had 2 degree of freedom, both lateral and torsional, to simulate the transmission of the strain at gear meshes nodes, where happens the transformation of twisting actions into lateral excitations, the responses on Gear Boxes bearings were low.

String Test conducted under very high densities conditions has confirmed an excellent mechanical train behavior, with low vibrations measured on all gear box bearings, 0.7 mils P-P (18 microns P-P) the maximum level recorded: this the evidence of a very predictable dynamic model used to validate gear-box lateral behavior and any potential lateral-torsional interaction.

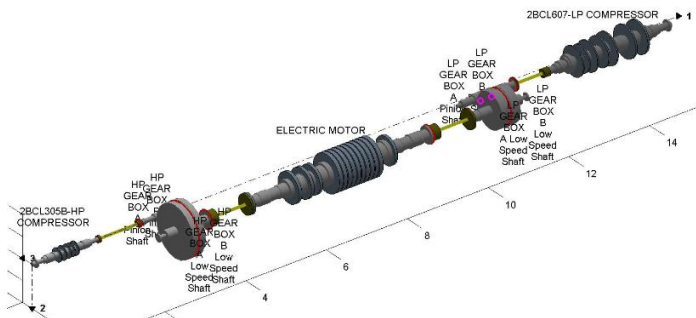


Figure 59. Torsional-Lateral train model

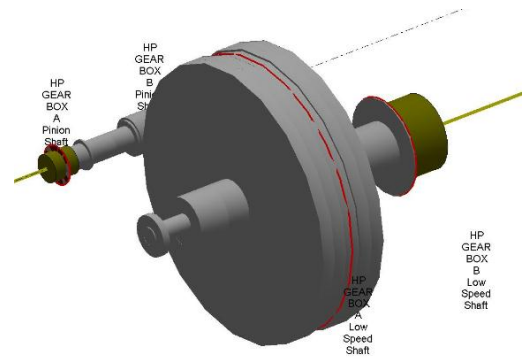


Figure 60. HP gear model

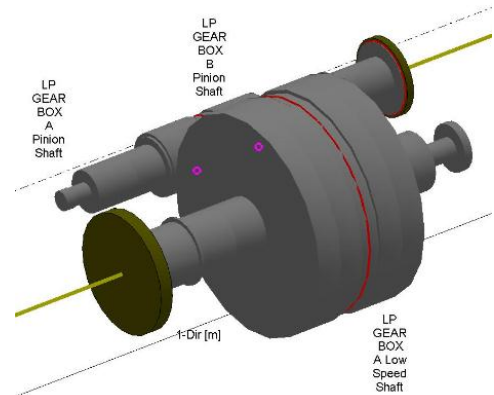


Figure 61. LP gear model

CONCLUSIONS

This paper describes of the design considerations in building the CO₂ compressors to be used at the Chevron-operated Gorgon Project.

The paper highlights the main technical features such as, driver-compressors architecture and comparison among alternatives, state of the art of CO₂ Equation of state, compressors aerodynamics, material selection, rotordynamics, sealing technologies, driver technologies, system integrations, maintenance and human factor requirements.

Complete test campaign main results are also described, resuming excellent mechanical behavior and very predictable thermodynamic models used to study CO₂ compressibility at very high pressure levels.

NOMENCLATURE

AF	= Amplification Factor
AGRU	= Acid gas removal unit
aMDEA	= Activated Methyl-diethanolamine
API	= American Petroleum Institute
ASME	= The American Society of Mechanical Engineers
C	= Damping matrix (diagonal, n by n), [kg·m ² /s]
C _{alt}	= Alternating Torque [N·m]
CCS	= Carbon capture and storage
C _p	= Specific Heat at constant pressure
C _v	= Specific Heat at constant volume

CO₂ = Carbon Dioxide
 DGS = Dry Gas Seals
 EOR = Enhanced oil recovery
 EOS = Equation of state
 FEA = Finite Element Analysis
 FSFL = Full Speed Full Load Full Pressure
 G = Spacer stiffness [N•m/ Θ]
 HC = Honeycomb
 HP = High pressure
 J = Inertia matrix (n by n), [kg•m²]
 JB = Journal bearing
 K = Stiffness matrix (n by n), [kg•m²/s²]
 LETDF = Low Emissions Technology Demonstration Fund
 LP = Low Pressure
 LNG = Liquefied Natural Gas
 Θ = Angular displacement vector (n by 1), [radian]
 M = applied moment vector (n by 1)
 MCS = Maximum Continuous Speed
 MRT = Mechanical Running Test
 N₂ = Nitrogen
 NEMA = National Electrical Manufacturer Association
 NIE = Notch Impact Energy
 O&G = Oil & Gas
 OEM = Original Equipment Manufacturer
 P&ID = Process and Instrument Diagram
 PWM = Pulse Width Modulation
 P-P = Peak To Peak
 PTC = Performance Test Code
 rpm = Revolutions Per Minute
 SCC = Stress corrosion cracking
 SoS = Speed of Sound
 T = Temperature
 UVT = Unbalance Verification Test
 VFD = Variable Frequency Driver

REFERENCES

American Petroleum Institute, “Brushless Synchronous Machines – 500kVA and Larger”, API Standard 546, 2nd Edition.
 American Petroleum Institute, “Special Purpose Gear Units for Petroleum, Chemical and Gas Industry Services”, API Standard 613, 5th Edition.
 American Petroleum Institute, “Special Purpose Couplings for Petroleum, Chemical and Gas Industry Services”, API Standard 671 - 4th Edition.
 American Petroleum Institute, “Axial and Centrifugal Compressors and Expander-compressors for Petroleum, Chemical, and Gas Industry Service”, API Standard 617, 7th Edition.
 Baldassarre, L., Bergamini, L., Camatti, M., Pelagotti, A., Tesi, A., Centrifugal compressors and pumps for CO₂ applications.

Banchi, N., Berti, M., Bigi, M., Bresciani, S., De Iaco, M., Milone, F., 2010, “Carbon Capture & Sequestration GE Oil & Gas CO₂ Management System - Rio Oil & Gas.
 Bertolo, S., Sett/Oct 2009, “Four post-combustion CO₂ compression strategies compared”, *Carbon Capture Journal*.
 Botero, C., Finkenrath, M., Belloni, C., 2009, “Thermoeconomic Evaluation of CO₂ Compression, for Post-Combustion CO₂ Capture Applications”, GT2009-60217.
 Chioetto S., Sivapuram, C., 2006 “Design, operation and re-rate consideration for integrally geared turbocompressors”, ImechE.
 Giovani, G., 2008, “Validation of Acid gas thermodynamic calculation model”.
 Navy Department, “Military standard mechanical vibrations of mechanical equipment MIL-STD 167 (SHIPS)”.
 NACE MR-0175 International, the Corrosion Society, “Petroleum and natural gas industries. Materials for use in H₂S containing environments in oil and gas production”.
 Robb, D., Sett/Oct 2009, “The exploding interest in CO₂”, *Turbomachinery Magazine*.
 Span, R., Wagner, W., 1996, “A new Equation of State for Carbon Dioxide Covering the Fluid region from Triple point temperature to 1100k at pressures up to 800 Mpa”, *Journal of Physical and Chemical Reference Data*, Vol. 25, No. 6.

ACKNOWLEDGEMENTS

The authors would like to acknowledge the colleagues of the entire GE Oil & Gas Engineering Department (Florence, Italy), for their extensive contributions during all engineering phase.
 We would also like to thank members of Chevron, Kellogg (London, UK) and KBR (Houston, USA) technical staff for their efforts, continuous support, precious contribution and suggestions.
 Finally, the authors want to thank GE Oil & Gas (Florence, Italy), Chevron, Kellogg (London, UK) and KBR (Houston, USA) companies for the great opportunity given to publish this article.